

A Graphical Correlation-Based Method for Counting the Number of Global 8-Cycles on the SCRAM Three-Layer Tanner Graph

Sally Nafie, Joerg Robert, Albert Heuberger

Lehrstuhl für Informationstechnik mit dem Schwerpunkt Kommunikationselektronik (LIKE)

Friedrich-Alexander Universität Erlangen-Nürnberg (FAU), 91058 Erlangen, Germany

{sally.nafie, joerg.robert, albert.heuberger}@fau.de

This work has been submitted to the IEEE for possible publication. Copyright may be transferred without notice, after which this version may no longer be accessible.

Abstract—This paper presents a novel graphical approach that counts the number of global 8-cycles on the SCRAM three-layer Tanner graph. SCRAM, which stands for Slotted Coded Random Access Multiplexing, is a joint decoder that meets challenging requirements of 6G. At the transmitter side, the data of the accommodated users is encoded by Low Density Parity Check (LDPC) codes, and the codewords are transmitted over the shared channel by means of Slotted ALOHA. Unlike the state-of-the-art sequential decoders, the SCRAM decoder jointly resolves collisions and decodes the LDPC codewords, in a similar analogy to Belief Propagation on a three-layer Tanner graph. By leveraging the analogy between the two-layer Tanner graph of conventional LDPC codes and the three-layer Tanner graph of SCRAM, the well-developed analysis tools of classical LDPC codes could be utilized to enhance the performance of SCRAM. In essence, the contribution of this paper is three-fold; First it proposes the methodology to utilize these tools to assess the performance of SCRAM. Second, it derives a lower bound on the shortest cycle length of an arbitrary SCRAM Tanner graph. Finally, the paper presents a novel graphical method that counts the number of cycles of length that corresponds to the girth.

Index Terms—Internet of Things; IoT; Internet of Everything; IoE; Machine to Machine; M2M; 6G; Low Density Parity Check Codes; LDPC; Slotted ALOHA; Coded Slotted ALOHA; Random Access; Belief Propagation; Tanner Graphs; Ultra-Reliable Low-Latency; URLLC

I. INTRODUCTION

The emerging 6G technology is provisioned to provide a wide spectrum of services and use cases such as Further enhanced Mobile Broadband (FeMBB), Extremely-Reliable Low-Latency Communication (ERLLC), ultra-massive Machine Type Communications (umMTC), Long-Distance High-Mobility Communications (LDHM), and Extremely-Low-Power Communications (ELPC) [1], in addition to numerous services that fall under the umbrella of Internet of Everything (IoE) [2]. The diverse services and use cases, expected to be supported by 6G impose challenges on the wireless systems, in terms of massive connectivity, reliability, latency, and complexity [3].

The state-of-the-art techniques resort to Non-Orthogonal Multiple Access (NOMA) [4]–[6] as a leading approach adopted in 5G to support overloading. NOMA schemes are classified into Power Domain (PD) and Code Domain (CD) NOMA [7]. In PD-NOMA [8]–[10], the system exploits the power-domain as the key ingredient that differentiates the users. Alternatively, NOMA schemes could be designed in the code domain, where each user is assigned different code

[11], [12]. In the literature, two viable CD-NOMA schemes are presented; Pattern Division Multiple Access (PDMA) [13] and Sparse Code Multiple Access (SCMA) [14].

In order to support overloading, NOMA schemes rely on thoroughly coordinating the resource allocation among the users. Consequently, these techniques perform poorly in terms of scalability. To ensure reliability, most of the proposed schemes adopt repetition coding [15], or a concatenation of repetition codes with more sophisticated Forward Error Correction (FEC) codes [16]. According to coding theory, repetition coding does not make the best use of the resources. To meet the low-latency constraint, some CD-NOMA schemes suggest a grant-free variant of their proposed scheme [17]. However, because these schemes strongly rely on coordinating the collisions, a grant-free scheme thereof is provisioned to deteriorate the performance. The techniques [18], [19] transmit replicas of the encoded packets by means of Random Access. These techniques not only lose the degrees of freedom because of the repetition coding, but also do not support overloading as the number of repetitions corresponds to the number of adopted users.

At the receiver side, the state-of-the-art NOMA schemes adopt a sequential decoding structure, portrayed in a Multiuser Detector (MUD) block that resolves the collisions, followed by a bank of FEC decoders to decode the adopted FEC code [20]–[23]. Some schemes tend to further optimize their decoding performance by adopting Turbo-like decoders which are also known as Iterative Detection and Decoding (IDD) [24]. Such decoding structure suggests extending a feedback link between the output of the the bank of FEC decoders and the input of the MUD detector. In essence, IDD could be regarded as an iterative sequential decoder.

In [25], a novel approach dubbed SCRAM is proposed. SCRAM, which stands for Slotted Coded Random Access Multiplexing, is a hybrid joint decoder, that combines the ultra-low latency privilege of Slotted ALOHA (SA) [26], with the robust performance of Low Density Parity Check (LDPC) codes [27]. At the transmitter side, the data of the various users are encoded by means of LDPC codes, and the codewords are transmitted over the shared channel by means of SA. The uncoordinated access results in collisions among the transmitted packets. Unlike the sequential decoders presented in the literature, the essence of the hybrid SCRAM decoder

lies in its ability to jointly resolve the collisions, and decode LDPC, in a similar fashion to Belief Propagation (BP) [28] on a joint three-layer Tanner graph.

Due to the analogy between the two-layer Tanner graph [29] representation of LDPC codes, and the three-layer Tanner graph of the proposed SCRAM, conventional methods that analyze the performance of classical LDPC codes, could be adopted to analyze and further optimize the performance of the proposed SCRAM. In classical LDPC codes, a visible error floor in the PER performance at high SNR region is caused by the presence of cycles in the adjacent Tanner graph [30].

Numerous techniques are proposed in the literature to assess the cycle profile of classical LDPC codes. By mapping the three-layer Tanner graph of SCRAM, these techniques could be adopted to analyze the cycle profile SCRAM. However, the complexity of these techniques, when adopted for SCRAM, grow exponentially in both the number of accommodated users, and the deployed LDPC codeword lengths. For that reason, this paper presents a thorough analysis tailored to the SCRAM three-layer Tanner graph, in addition to a derivation of the shortest cycle length, known as the girth. In essence, the detailed analysis is utilized to design a graphical approach that quantifies the number of cycles of girth length, on any arbitrary SCRAM Tanner graph.

The rest of this paper is organized as follows. Section II covers the system model of SCRAM. In Section III, the utilization of the cycle counting algorithms of classical LDPC codes, in conjunction with SCRAM is tackled. In Section IV, a detailed analysis of the SCRAM three-layer Tanner graph is presented, in addition to the derivation of the SCRAM girth. Section V proposes a novel graphical algorithm that quantifies the number of cycles whose length equals to the girth. Moreover, Section VI shows the results of the proposed graphical method. Finally, Section VII summarizes the paper and sheds light on the potential future implications.

II. SCRAM PRELIMINARIES

A. System Model

The Hybrid SCRAM system incorporates N_u users sharing the SA wireless medium. Each user U_{n_u} , $\forall n_u = 1, \dots, N_u$, has an information packet, $\mathbf{b}^{(n_u)}$, of length k_{n_u} bits. This packet is encoded with an LDPC encoder, of code rate $r_{n_u} = k_{n_u}/n_{n_u}$, producing an output codeword, $\mathbf{c}^{(n_u)}$, of length n_{n_u} bits. Without loss of generality, the encoded bits are mapped to BPSK modulated symbols. The vector of modulated symbols of user U_{n_u} , is given by $\mathbf{x}^{(n_u)}$. The BPSK symbols are then to be transmitted using OFDM. Incorporating OFDM is twofold: to provide slot synchronization due to the gridded analogy between SA and OFDM subcarriers, and to translate the multipath fading channel to multiple flat fading subchannels. Prior to transmission, each user, U_{n_u} , randomly and independently chooses n_{n_u} SA slots (OFDM subcarriers) to transmit its modulated encoded codeword. Let N_s denote the total number of available slots per SA frame. In this case, the channel load – defined as the number of useful information bits per SA slot – is given by $D = \sum_{n_u=1}^{N_u} k_{n_u}/N_s$.

At the receiver side, a joint decoding of the contended LDPC codewords is performed iteratively. Unlike the sequential decoders presented in the literature, the

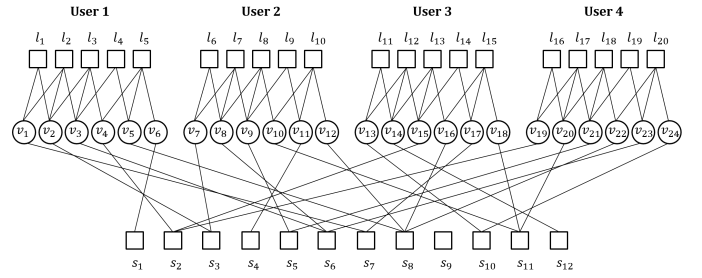


Fig. 1. Three-Layer Tanner graph example of SCRAM system with $N_u = 4$ users, each transmitting $n_{n_u} = 6$ LDPC encoded symbols over a system with $N_s = 12$ SA slots

SCRAM mechanism incorporates a joint three-layer Tanner graph that allows for the joint decoding. The idea is inspired by BP decoding of graph-based codes such as LDPC codes.

B. Three-Layer Tanner Graph Representation

Assuming a SCRAM system that accommodates N_u users, the corresponding joint three-layer Tanner graph comprises a set of variable nodes representing the transmitted symbols from all the users. These variable nodes are bounded by two layers of check nodes. The first check nodes layer corresponds to the slots of the shared SA medium. The other layer is driven from the conventional parity check nodes in the BP decoding of LDPC codes. Let N_v denote the number of variable nodes. Each transmitted symbol is represented by a variable node.

Thus, $N_v = \sum_{n_u=1}^{N_u} n_{n_u}$, where n_{n_u} represents the number of transmitted symbols of user U_{n_u} per SA frame. The number of SA check nodes, denoted by N_s , is allocated according to the available resources. The total number of LDPC check nodes is given by $N_l = \sum_{n_u=1}^{N_u} m_{n_u}$, where $m_{n_u} \geq n_{n_u} - k_{n_u}$, denotes the number of LDPC parity check equations of user U_{n_u} .

The edges connecting the variable nodes and the SA check nodes depend on the random selection of the transmission slots of each user. This means that a contended SA check node can be connected to more than one variable node. Meanwhile, the connections of the variable nodes to the LDPC check nodes are fully determined by the deployed LDPC encoder at each user's transmit terminal.

For illustration, consider the three-layer Tanner graph of the SCRAM model shown in Figure 1. The model incorporates $N_u = 4$ users, each transmitting $n_{n_u} = 6$ modulated symbols. It is assumed that the four users adopt identical LDPC encoders with $n_{n_u} = 6$ variable nodes, and $m_{n_u} = 5$ LDPC check nodes, per user. This means that the three-layer Tanner graph of such a model consists of $N_v = 24$ variable nodes, $N_l = 20$ LDPC check nodes. Moreover, the graph has a set of $N_s = 12$ SA check nodes, that correspond to 12 allocated frequency subcarriers. It is also assumed that each user blindly selects six subcarriers to transmit its six modulated symbols.

C. Iterative Joint SCRAM Decoding

Algorithm 1 depicts the steps of the joint SCRAM scheme for one decoding iteration. The variable nodes concurrently communicate with both the SA and the LDPC check nodes, on the three-layer Tanner graph that comprises N_v variable nodes, N_s SA check nodes, and N_l LDPC check nodes.

1) *Check Nodes to Variable Nodes:* In the first half of the iteration, the SA and LDPC check nodes calculate their provisioned Log Likelihood Ratios (LLRs), and send them to their corresponding variable nodes.

a) *SA Check Nodes to Variable Nodes:* The SA check node update is illustrated in steps 1 through 13, such that S_{n_s, n_v} represents the LLR transmitted from SA check node s_{n_s} to variable node v_{n_v} , if v_{n_v} belongs to the set $A_{s_{n_s}}$, of connected variable nodes to SA check node s_{n_s} . Assuming $V_{n_s, n_v}^{(S)}$ denotes the LLR that SA check node s_{n_s} received from its corresponding variable node v_{n_v} in the previous iteration, in step 10, s_{n_s} , calculates the conditional probability of the received signal given every possible combination of its collided symbols. In steps 5 through 9, SA check node s_{n_s} , computes the joint apriori probability of these vector combinations, while steps 3 and 4 calculate the probability of the individual elements within these vectors.

The following notations are adopted. For $n_s = 1, \dots, N_s$, y_{n_s} represents the channel received signal at SA slot s_{n_s} . Moreover, $M_{n_s}^{(\pm)}$ denotes the cardinality of the set of possible vectors of all the collided symbols at SA check node s_{n_s} , that assume that the symbol represented by variable node v_{n_v} is +1 and -1, respectively. For $m = 1, \dots, M_{n_s}^{(\pm)}$, let $\tilde{\mathbf{x}}_m^{(n_v, +1)}$ and $\tilde{\mathbf{x}}_m^{(n_v, -1)}$ be a vector that corresponds to one of the $M_{n_s}^{(\pm)}$ combination vectors, that assume that the symbol represented by v_{n_v} is +1 and -1, respectively. Furthermore, $P(\tilde{\mathbf{x}}_m^{(n_v, +1)})$ and $P(\tilde{\mathbf{x}}_m^{(n_v, -1)})$ denote the apriori probability of the vectors $\tilde{\mathbf{x}}_m^{(n_v, +1)}$ and $\tilde{\mathbf{x}}_m^{(n_v, -1)}$, respectively. In addition, $\tilde{x}_{m, d}^{(n_v, +1)}$ and $\tilde{x}_{m, d}^{(n_v, -1)}$ represent a possible value for the modulated symbol represented by the d^{th} variable node that collides at SA check node s_{n_s} , in the vector $\tilde{\mathbf{x}}_m^{(n_v, +1)}$ and $\tilde{\mathbf{x}}_m^{(n_v, -1)}$, respectively. Moreover, $h_{s_{n_s}, d}$ denotes the estimated fading coefficient of the channel between SA check node s_{n_s} and the d^{th} variable node that collides at it. Finally, σ^2 is the noise variance of the complex AWGN channel.

b) *LDPC Check Nodes to Variable Nodes:* Inspired by BP decoding of classical LDPC codes, Steps 14 through 18 give the LDPC check node update, such that L_{n_l, n_v} , represents the LLR to be transmitted from LDPC check node l_{n_l} , to variable node v_{n_v} , while $V_{n_l, n_v}^{(L)}$ represents the LLR received by LDPC check node l_{n_l} from variable node v_{n_v} , in the previous iteration. Moreover, $A_{l_{n_l}}$ denotes the set of variable nodes connected to LDPC check node l_{n_l} .

2) *Variable Nodes to Check Nodes:* Upon receiving the LLRs from the SA and LDPC check nodes, the variable nodes calculate new LLRs to be transmitted to their corresponding check nodes, both SA and LDPC, in the next half of the iteration. Steps 19 through 24 highlight the variable node update, such that $V_{n_l, n_v}^{(L)}$ and $V_{n_s, n_v}^{(S)}$ represent the information transmitted from variable node, v_{n_v} to LDPC check node l_{n_l} , and SA check node s_{n_s} , respectively. Moreover, L_{n_l, n_v} and S_{n_s, n_v} represent the LLR, that variable node, v_{n_v} , has received in the first half of the iteration from LDPC check node, l_{n_l} , and SA check node, s_{n_s} , respectively. Furthermore, $A_{v_{n_v}}^{(L)}$ and $A_{v_{n_v}}^{(S)}$, respectively denote the set of LDPC check nodes, and the set of SA check nodes, connected to variable node v_{n_v} .

Algorithm 1 Joint SCRAM Decoding

//SA Check Node Update

1: **for** $n_s = 1 : N_s$ **do**

2: **for** $n_v \in A_{s_{n_s}}$ **do**

3:
$$P\left(\tilde{x}_{m, d}^{(n_v, +1)}\right) = \frac{1}{1 + \exp\left[-V_{n_s, n_v}^{(S)}\right]}$$

4:
$$P\left(\tilde{x}_{m, d}^{(n_v, -1)}\right) = \frac{-V_{n_s, n_v}^{(S)}}{1 + \exp\left[-V_{n_s, n_v}^{(S)}\right]}$$

5: **if** $iter \equiv 1$ **then**

6:
$$P(\tilde{\mathbf{x}}_m^{(n_v, \pm 1)}) = \frac{1}{M_{n_s}^{(\pm)}}$$

7: **else**

8:
$$P(\tilde{\mathbf{x}}_m^{(n_v, \pm 1)}) = \prod_{\substack{d=1 \\ v_{n_v} \neq v_{s_{n_s}, d}}}^{d_{s_{n_s}}} P\left(\tilde{x}_{m, d}^{(n_v, \pm 1)}\right)$$

9: **end if**

10:
$$P\left(y = y_{n_s} | \tilde{\mathbf{x}}_m^{(n_v, \pm 1)}\right) =$$

$$\frac{1}{\pi \sigma^2} \exp\left[\frac{1}{\sigma^2} \cdot \left| y_{n_s} - \sum_{d=1}^{d_{s_{n_s}}} h_{s_{n_s}, d} \tilde{x}_{m, d}^{(n_v, \pm 1)} \right|^2\right]$$

11:
$$S_{n_s, n_v} = \ln \frac{\sum_{m=1}^{M_{n_s}^{(+)}} \left[P(y=y_{n_s} | \tilde{\mathbf{x}}_m^{(n_v, +1)}) \cdot P(\tilde{\mathbf{x}}_m^{(n_v, +1)}) \right]}{\sum_{m=1}^{M_{n_s}^{(-)}} \left[P(y=y_{n_s} | \tilde{\mathbf{x}}_m^{(n_v, -1)}) \cdot P(\tilde{\mathbf{x}}_m^{(n_v, -1)}) \right]}$$

12: **end for**

13: **end for**

//LDPC Check Node Update

14: **for** $n_l = 1 : N_l$ **do**

15: **for** $n_v \in A_{l_{n_l}}$ **do**

16:
$$L_{n_l, n_v} = -2 \tanh^{-1} \left(\prod_{\substack{v_{n_v'} \in v_{l_{n_l}} \\ v_{n_v'} \neq v_{n_v}}} \tanh \left(-\frac{V_{n_l, n_v'}^{(L)}}{2} \right) \right)$$

17: **end for**

18: **end for**

//Variable Node Update

19: **for** $n_v = 1 : N_v$ **do**

20: **for** $n_l \in A_{v_{n_v}}^{(L)}, n_s \in A_{v_{n_v}}^{(S)}$ **do**

21:
$$V_{n_l, n_v}^{(L)} = \sum_{\substack{s_{n_s'} \in s_{v_{n_v}} \\ s_{n_s'} \neq s_{n_s}}} S_{n_s', n_v} + \sum_{\substack{l_{n_l'} \in l_{v_{n_v}} \\ l_{n_l'} \neq l_{n_l}}} L_{n_l', n_v}$$

22:
$$V_{n_s, n_v}^{(S)} = \sum_{\substack{s_{n_s'} \in s_{v_{n_v}} \\ s_{n_s'} \neq s_{n_s}}} S_{n_s', n_v} + \sum_{l_{n_l'} \in l_{v_{n_v}}} L_{n_l', n_v}$$

23: **end for**

24: **end for**

III. CYCLE-PROFILE OF SCRAM

On a Tanner graph, a cycle is defined as a path that starts and terminates at the same node, and goes through a sequence of nodes via their connected edges [30]. For the path to be called a cycle, the edges, and all the nodes except the terminal ones have to be distinct. If the first edge in the path is the same as the last edge, the path is rather referred to as a closed walk, and is not considered a cycle [30]. A cycle of length L is simply referred to as an L -cycle. The girth of a Tanner graph is denoted by g , and is defined as the length of the shortest cycle within the graph [31]. A cycle profile is a quantitative analysis of the number of short cycles within a Tanner graph. These short cycles are namely those whose length is less than double the girth [30].

A. Cycle-Profile of Classical LDPC Codes

An (n, k) LDPC code is fully described by a Tanner graph that comprises n variable nodes, and $m \geq n - k$ check nodes [32]. The presence of short cycles in the Tanner graph hinders the performance of BP, and leads to error propagation [33]. For that purpose, many algorithms that quantify and evaluate the cycle profile of a given LDPC code were proposed.

Two algorithms are chosen in the sequel for evaluating the cycle profile of a given LDPC code, and later for extending the analysis to the three-layer Tanner graph of SCRAM. The first algorithm [30] adopts an iterative message-passing algorithm, that tracks for every node within the Tanner graph, the number of iterations required by a monomial variable to make a full-cycle back to this initiating node. The second algorithm [31] debates that a cycle that starts and ends at one node, can be traced at an intermediate point half-way within the cycle length. These two algorithms are going to be referred to as Full-Cycle and Half-Cycle counting algorithms, respectively.

1) *Full-Cycle Algorithm*: To calculate the number of cycles of particular length that pass through a specific node, the algorithm is initialized at $t = 0$, by allowing this node to transmit a different monomial (dummy variable of unit power) over each of its connected edge, while all the other nodes within the set would send unity. The message passing algorithm is activated, where at every time instant, only one set of nodes is active and is allowed to pass information to the corresponding set of nodes. The information that a node passes on any of its connected edges corresponds to the multiplication of all its incoming messages at the previous time instant, except the incoming message on the edge that the node would send back on. If the node of interest is involved in a cycle of length L , it will receive copies of its transmitted monomials, at different edges, first at $t = L - 1$.

If the node of interest receives N copies of its transmitted monomials, on different edges, at a certain time instant, t , this indicates that this node is involved in N cycles of length $L = t + 1$. These are referred to as $N_L(v_i)$ or $N_L(l_j)$, depending on whether the node of interest is a variable node $v_i, \forall i = 1, \dots, n$, or a check node $l_j, \forall j = 1, \dots, m$, respectively. The process is repeated for all the nodes within one set of nodes. For example, looping over the variable nodes for $i = 1, \dots, n$, where n is the total number of variable nodes, yields the number of cycles, $N_L(v_i)$, of length L , that pass through variable node v_i . After that, the results are accumulated in a global counter, C_L , that corresponds to all the cycles of length L , that pass through all the variable nodes.

Figure 2 depicts the steps of the Full-Cycle algorithm, to calculate the cycles that pass through variable node v_3 . The algorithm is initiated at $t = 0$, where v_3 sends X_1 , X_2 , and X_3 , along its first, second, and third edges, respectively. All the other variable nodes would send unities. At $t = 1$, the check nodes gather the information they collect along their connected edges, in order to calculate the updated information that they send back. For example, check node l_2 , receives 1, 1, and X_1 , along its first, second, and third edges, respectively. At $t = 1$, l_2 sends back X_1 , X_1 , and 1, along its first, second, and third edges, respectively. At $t = 2$, and $t = 3$, extrinsic information is passed from variable nodes to check nodes, and from check nodes to variable nodes, respectively. Because

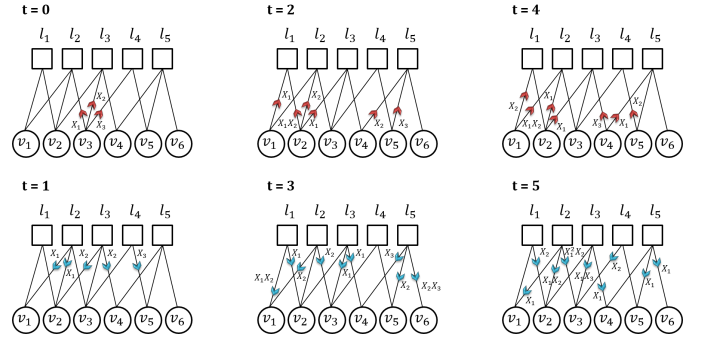


Fig. 2. Example of Full-Cycle Algorithm on a Tanner graph of $n = 6$ variable nodes and $m = 5$ check nodes, counting the cycles that pass through variable node v_3

at $t = 3$, v_3 receives one copy of X_2 along its first edge, and one copy of X_1 along its first edge, one cycle of length $L = t + 1 = 4$ is declared. This means that $N_4(v_3) = 1$. At $t = 4$, the variable nodes pass their extrinsic information to their connected check nodes, while v_3 passes only unities. In return, at $t = 5$, the check nodes update their extrinsic information, and send them back to their corresponding variable nodes. This time, v_3 receives again copies of its monomials at $t = 5$, which indicates that there is one or more cycles of length $L = 6$. On its first edge, v_3 receives $X_1^2 X_2$. It discards X_1^2 , as it corresponds to copies of X_1 , which is the initially transmitted monomial on the first edge of v_3 . This leaves v_3 with one copy of X_2 on its first edge. On the second edge, v_3 receives $X_1 X_3$, which corresponds to one copy of X_1 and one copy of X_3 , none of which should be discarded. On the third edge, v_3 receives a copy of X_2 , which should be kept. In total, at $t = 5$, v_3 has a copy of X_1 , two copies of X_2 , and a copy of X_3 . This sums up to four, meaning that the total number of cycles of length $L = t + 1 = 6$, that pass through v_3 is $4/2 = 2$. That is, $N_6(v_3) = 4$.

Because v_3 has one cycle of length four, the girth of this Tanner graph is four. Thus, the algorithm counts all cycles of length up to $2g - 2 = 6$. For v_3 , the number of 4-cycles, $N_4(v_3)$, and the number of 6-cycles, $N_6(v_3)$ should be accumulated on the global 4-cycle counter, C_4 , and the global 6-cycle counter, C_6 , respectively. Finally, v_3 and its three edges should be deleted from the graph to avoid duplications.

2) *Half-Cycle Algorithm*: The essence of the Half-Cycle counting algorithm lies in its ability to get rid of half of the cycle round while adopting the message passing algorithm to trace the cycles. It debates that because a typical LDPC cycle on the Tanner graph starts and terminates at the same node, the cycle could be traced half-way. In essence, the algorithm is able to count the number of cycles on a given Tanner graph, yielding the same results as the Full-Cycle algorithm proposed in [30], at half the required computational complexity.

3) *Cycle Profile Analysis of a Classical LDPC Code*: This section analyzes the cycle profile of the (4320, 2160) LDPC code, proposed in the DVB-NGH standard [34]. Table I shows the cycle profile of the NGH LDPC code, obtained from either the Full-Cycle, or the Half-Cycle algorithm, which yields exactly the same results. Because the Half-Cycle algorithm requires half the computational complexity of the Full-Cycle

TABLE I
CYCLE PROFILE OF (4320, 2160) DVB-NGH LDPC CODE

	C_6	C_8	C_{10}
(4320, 2160) DVB-NGH LDPC	31200	1558340	73706359

algorithm, in the sequel, only the Half-Cycle algorithm would be utilized. The girth of the NGH code is found by the algorithm to be six. Consequently, the algorithm could quantify the number of cycles, whose length is less than or equal ten. As shown in the table, the analysis indicate that the NGH code has $C_6 = 31200$, cycles of length six, $C_8 = 1558340$, cycles of length eight, and $C_{10} = 73706359$, cycles of length ten.

B. SCRAM as a Hybrid Matrix

There is a one-to-one relationship between the adjacent parity check matrix of an LDPC code, and its corresponding Tanner graph. Belief Propagation decoding of LDPC codes incorporates the traverse of soft information back and forth on the Tanner graph between the variable nodes and the check nodes. In a similar fashion, for the SCRAM decoder, the soft information traverses the three-layer Tanner graph back and forth between variable nodes, and both SA and LDPC check nodes. Inspired by LDPC, a one-to-one relationship between the SCRAM three-layer Tanner graph, and an adjacent hybrid matrix that fully describes the joint decoder, is proposed.

An (n, k) LDPC code, with k information bits, and n coded bits, is described by a two-layer Tanner graph that comprises n variable nodes, and $m \geq n - k$ LDPC check nodes. The adjacent parity check matrix, \mathbf{H} , of such code consists of n columns that correspond to the set of variable nodes, and m rows that correspond to the LDPC check nodes. A SCRAM system that incorporates N_u users, is modeled on a three-layer Tanner graph, with a set of variable nodes encompassed by two sets of check nodes; SA and LDPC check nodes. For $n_u = 1, \dots, N_u$, if user U_{n_u} adopts an (n_{n_u}, k_{n_u}) LDPC code, then the three-layer Tanner graph comprises a set of $N_v = \sum_{n_u=1}^{N_u} n_{n_u}$ variable nodes, a set of $N_l = \sum_{n_u=1}^{N_u} m_{n_u}$ LDPC check nodes, and a set of N_s SA check nodes, that correspond to the N_s slots allocated for transmission.

Similar to conventional LDPC codes, the columns of the proposed hybrid matrix represent the set of variable nodes in the three-layer Tanner graph. This means that the SCRAM hybrid matrix, $\mathbf{H}_{\text{SCRAM}}$, consists of $N_v = \sum_{n_u=1}^{N_u} n_{n_u}$ columns, that represent the set of N_v variable nodes from the three-layer Tanner graph. The i^{th} symbol of user U_{n_u} , such that $1 \leq n_u \leq N_u$, and $1 \leq i \leq n_{n_u}$, corresponds to the n_v^{th} column of $\mathbf{H}_{\text{SCRAM}}$, such that $n_v = \left(\sum_{n_u=1}^{n_u-1} n_{n_u} \right) + i$.

The first N_s rows of $\mathbf{H}_{\text{SCRAM}}$ correspond to the N_s SA check nodes in the three-layer Tanner graph, or alternatively the N_s frequency subcarriers allocated for transmission. The population of this part of the matrix depends on the randomly-selected slots by each of the N_u users, to transmit its n_{n_u} modulated symbols. For $n_s = 1, \dots, N_s$, $n_u = 1, \dots, N_u$, and $i = 1, \dots, n_{n_u}$, if user U_{n_u} selects SA slot s_{n_s} to transmit its i^{th} modulated symbol, an entry of 1 is placed at

the intersection of row n_s , and column n_v in $\mathbf{H}_{\text{SCRAM}}$, such that $n_v = \left(\sum_{n_u=1}^{n_u-1} n_{n_u} \right) + i$.

The next set of rows in $\mathbf{H}_{\text{SCRAM}}$ corresponds to the vertical concatenation of the N_l LDPC check nodes of the three-layer Tanner graph. This means that for $n_u = 1, \dots, N_u$, the m_{n_u} LDPC check nodes of user U_{n_u} , correspond to the m_{n_u} rows of $\mathbf{H}_{\text{SCRAM}}$, that are located at row indices $N_s + \left(\sum_{n_u=1}^{n_u-1} m_{n_u} \right) + 1$ to $N_s + \left(\sum_{n_u=1}^{n_u-1} m_{n_u} \right) + m_{n_u}$. The population of this part of the matrix is deterministic, and depends fully on the location of ones in the parity check matrix, \mathbf{H}_{n_u} , of the adopted LDPC code of user U_{n_u} , for $n_u = 1, \dots, N_u$. This means that if user U_{n_u} adopts an LDPC code, described by a parity check matrix, \mathbf{H}_{n_u} , that has an entry of 1, at the intersection of column i , for $i = 1, \dots, n_{n_u}$, and row j , for $j = 1, \dots, m_{n_u}$, this entry is mapped to an entry of 1, at the intersection of column $\left(\sum_{n_u=1}^{n_u-1} n_{n_u} \right) + i$, and row $N_s + \left(\sum_{n_u=1}^{n_u-1} m_{n_u} \right) + j$ in $\mathbf{H}_{\text{SCRAM}}$.

For illustration, consider again the three-layer Tanner graph example shown in Figure 1. The hybrid matrix of this model is depicted in Figure 3. The matrix consists of $N_v = 24$ columns representing the variable nodes, and $N_s + N_l = 32$ rows representing both the SA and the LDPC check nodes. The location of the 1s in the upper SA submatrix (first 12 rows) depends entirely on the random access selection of the users. For example, the Tanner graph shows connections between the six modulated symbols of user U_1 , and SA slots s_7, s_3, s_6, s_2, s_8 , and s_1 . This maps to six entries of 1 at the intersection of the first six columns of $\mathbf{H}_{\text{SCRAM}}$, and the corresponding row indices of the selected SA slots. The blank entries in the matrix simply denote the absence of connections, and could also be represented by zeros.

The next 20 rows of $\mathbf{H}_{\text{SCRAM}}$ correspond to the vertical concatenation of the five LDPC check nodes of each of the four users. Each user possesses connections only to its own set of LDPC check nodes. This is demonstrated in the block-wise staircase fashion in the lower LDPC submatrix of $\mathbf{H}_{\text{SCRAM}}$. Within the block zone of a specific user, the entries are regulated by the location of ones in the parity check matrix of the adopted LDPC code of that user. For example, the second variable node of user U_3 is connected to its first, second, and third LDPC check nodes. On $\mathbf{H}_{\text{SCRAM}}$, this is translated to three entries of 1 at the intersection of the 14th column and the 23rd, 24th, and 25th rows.

C. Cycle-Profile of SCRAM

The essence of mapping the joint SCRAM system to a hybrid matrix representation, lies in enabling the feeding of the mapped hybrid SCRAM matrix, to one of the discussed cycle counting algorithms (Full-Cycle [30] or Half-Cycle [31]), which in return yields both the girth, and the cycle profile of the mapped SCRAM system. Because the Half-Cycle algorithm requires only half the computational complexity, it is chosen as the candidate cycle-counting algorithm of the matrix representation of the SCRAM Tanner graph.

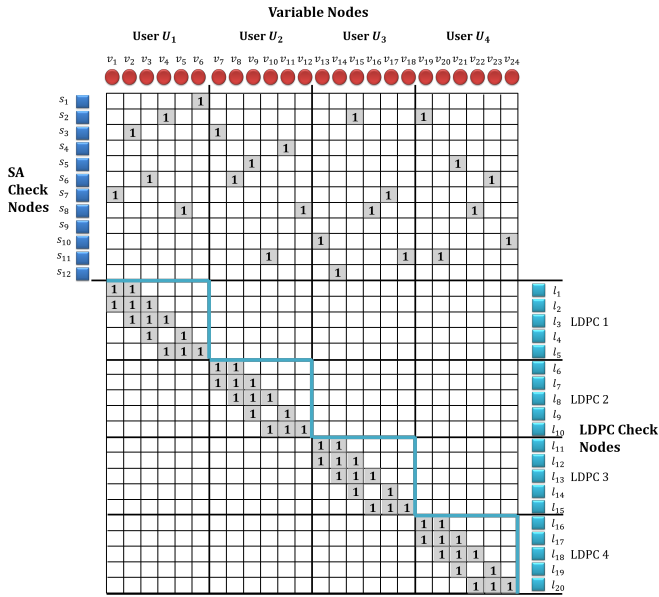


Fig. 3. Hybrid Matrix of a SCRAM system with $N_u = 4$ Users, each transmitting $n_{n_u} = 6$ LDPC encoded symbols over a system with $N_s = 12$ SA slots, by means of Random Access

TABLE II
CYCLE PROFILE OF SCRAM, WITH $N_u = 4$ USERS, ADOPTING THE (4320, 2160) DVB-NGH LDPC CODE, WITH RANDOM ACCESS OVER A CHANNEL WITH $N_s = 8640$ SLOTS

	C_6	C_8	C_{10}
(4320, 2160) DVB-NGH LDPC	31200	1558340	73706359
SCRAM, with $N_u = 4$ users	124800	6234085	

Table II depicts the cycle profile of a SCRAM system that accommodates $N_u = 4$ users, where each user deploys the (4320, 2160) DVB-NGH [34] LDPC code. The shared channel comprises $N_s = 8640$ frequency subcarriers. The three-layer Tanner graph is first mapped to hybrid SCRAM matrix, and fed to the Half-Cycle counting algorithm. The girth of the SCRAM systems was found by the algorithm to be six. Consequently, the Half-Cycle counting algorithm is capable of quantifying all short cycles of length up to ten. However, in order to reduce the computational complexity, the search was limited to finding only the cycles of length six and eight, as they are provisioned to have the more dominant impact on the systems' performance. For convenience, the table also includes the cycle profile of the classical DVB-NGH LDPC code, that was presented in Table I.

As shown in the table, the SCRAM system possesses $C_6 = 124800$ cycles of length six, and $C_8 = 6234085$ cycles of length eight. A careful inspection reveals that the total number of 6-cycles in the joint SCRAM system, is four times the number of 6-cycles in the pure LDPC case. This implies that the only source of 6-cycles, on the three-layer Tanner graph of SCRAM, is the local cycles on the individual LDPC subgraphs of each of the four accommodated users.

IV. DERIVATION OF SCRAM GIRTH

In the following, a step-by-step analysis of the flow of beliefs on the three-layer Tanner graph of the proposed joint

SCRAM decoder is presented. Without loss of generality, the analysis is illustrated on the SCRAM example in Figure 1. However, the findings apply to any arbitrary SCRAM model. Because the purpose of is finding the girth of the SCRAM Tanner graph, during the analysis, any potential cycle with provisioned cycle length that exceeds the girth (so far found cycle with minimum length) will be discarded.

Two sub-definitions of cycles of the three-layer Tanner graph are declared; a local cycle and a global cycle. A local cycle on the SCRAM Tanner graph denotes a cycle that initiates and terminates at a given variable node, that belongs to a certain user, by means of traversing a path between variable nodes and LDPC check nodes that represent the LDPC code of the denoted user. A global cycle on the other hand, is defined as a cycle that initiates and terminates at a variable node, that belongs to a certain user, by means of traversing a path between variable nodes and LDPC check nodes that belong to different users, via trespassing their commonly connected SA check nodes.

Both the local cycles and global cycles are considered as cycles of the three-layer Tanner graph. Consequently, the overall girth of the SCRAM graph, is counted as the minimum cycle length of all the local and global cycles. The Half-Cycle algorithm could easily identify the girth of the local cycles. This can be achieved by passing the parity check matrices of the underlying LDPC codes of the N_u users, one at a time. For $n_u = 1, \dots, N_u$, let g_{n_u} be the calculated girth of the underlying LDPC code of user U_{n_u} , at the output of the Half-Cycle algorithm. The least local cycle length, g_{local} , is thus the minimum of all the N_u girths of the different LDPC codes. That is, $g_{local} = \min_{n_u} (g_{n_u})$.

More generally, passing the SCRAM hybrid matrix, \mathbf{H}_{SCRAM} , to the Half-Cycle algorithm could yield the overall girth, g_{SCRAM} , of the three-layer Tanner graph. However, the complexity of the algorithm grows extensively with the number of users, and the codeword length. The incentive of the analysis proposed herein, is to derive a lower-bound on the length, g_{global} , of the shortest global cycle in the graph. The overall girth, g_{SCRAM} , of the SCRAM graph would then be the minimum of the local girth, g_{local} , and the analyzed global girth, g_{global} .

Consider again the SCRAM example in Figure 1, with $N_u = 4$ users, $n_{n_u} = 6$ symbols per user, $m_{n_u} = 5$ LDPC check nodes per user, and $N_s = 12$ SA slots. As aforementioned, the four users adopt identical LDPC codes. The girth of each of the adopted LDPC codes was found to be four. That is, $g_{n_u} = 4 \forall n_u = 1, \dots, 4$. Thus, the minimum local girth is given by $g_{local} = 4$. In the following, the example is analyzed to track the shortest length of global cycles. For illustration, variable node v_3 is chosen as the initiating node of the belief. Hence, a full global cycle is declared when the belief traverses the three-layer Tanner graph all the way back to v_3 . Equivalently, any of the $N_v = 24$ variable nodes is a suitable candidate for the initiation of the message.

Figure 4 depicts in bold the initialization step at time instant $t = 0$, such that only variable node v_3 is active, and sends a monomial (e.g. X_1) concurrently in both directions to its adjacent SA check node, s_6 , and LDPC check nodes, l_2 , l_3 , and l_4 . The monomial transmitted to the LDPC check nodes

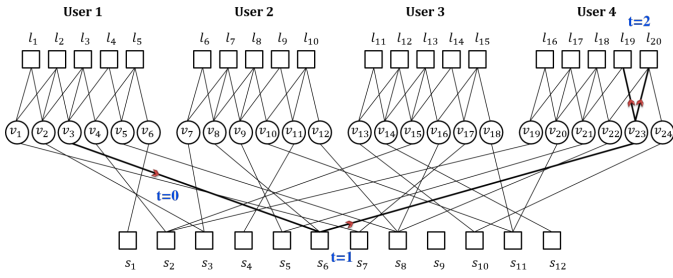


Fig. 4. Track of flow of beliefs at $t = 0, 1, 2$, on a SCRAM graph with $N_u = 4$ users, $n_{n_u} = 6$ symbols, and $N_s = 12$ slots

has two provisioned paths in the subsequent time instants. The first path is a local cycle between the variable nodes and LDPC check nodes that belong to the subgraph of user U_1 . The girth of such a local cycle can not go below the pre-calculated local girth, g_1 , of the underlying LDPC code of user U_1 . The second provisioned path of the monomials received at the LDPC check nodes, is that in the next time slot they flow from the LDPC check nodes to other variable nodes that belong to user U_1 . For example, LDPC check node, l_2 , would forward the monomial to variable nodes v_1 , and v_2 , which in return will forward the monomial to their respective SA check nodes. The global cycle analysis in this case would translate to finding the length of the cycles initiated from either v_1 or v_2 , in addition to the two extra time slots (or transitions), required for the monomial to hop from v_3 to l_2 till it lands on v_1 and v_2 . Because the main interest is to identify the shortest cycle length, this provisioned path is discarded as it yields a cycle of longer length. The only relevant transition at this time instant, is thus the transition from variable node v_3 to SA slot s_6 . Hence, for the subsequent analysis, the cycle will be traced further from s_6 .

At $t = 1$, SA check node s_6 forwards the monomial it received from variable node v_3 , at the previous time instant, to its adjacent variable nodes, v_8 , and v_{23} . The concept of extrinsic information prohibits s_6 from transmitting the monomial back to v_3 . Because the purpose is to analyze and find the shortest path, the idea could be fulfilled by means of tracking either v_8 or v_{23} . This statement would have been misleading, if the target was to calculate the number of cycles of length that is equal to the girth. However, for identifying the girth, considering one variable node only would be sufficient. Thus, in order to avoid confusion, for the rest of the analysis, the cycle is to be traced from v_{23} .

Figure 4 also shows the transition of the monomial from variable node v_{23} to its adjacent LDPC check nodes l_{19} and l_{20} at $t = 2$. Again, due to extrinsic message passing, the monomial can not be sent back from v_{23} to SA check node s_6 . Proceeding from this point, two different paths with different properties could be taken depends on whether the cycle is traced from l_{19} or from l_{20} . These two possibilities should be handled separately to avoid confusion. First, the path from l_{20} would be tracked for the subsequent time slots. The analysis would track the monomial after it is forwarded from l_{20} , all the way till it reaches v_3 . After that, the analysis would go back to this point in time, and track the path taken from l_{19} . These two cases of starting from l_{20} , and starting from l_{19} , would be denoted as case 1 and case 2, respectively.

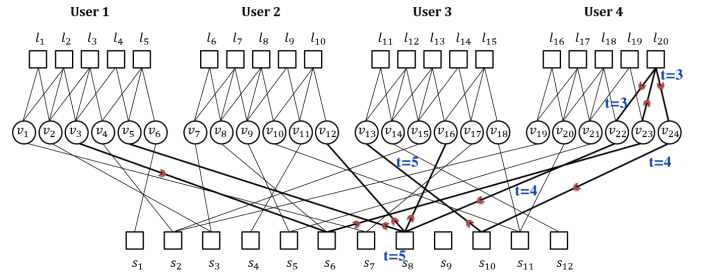


Fig. 5. Track of flow of beliefs at $t = 3, 4, 5$, Case 1, on a SCRAM graph with $N_u = 4$ users, $n_{n_u} = 6$ symbols, and $N_s = 12$ slots

At $t = 3$, as shown in Figure 5, for case 1, LDPC check node, l_{20} , forwards the monomial to its adjacent variable nodes v_{22} and v_{24} . These also yield different paths with different features that would be handled jointly. Consequently, for the next time slots, the analysis would continue from both v_{22} and v_{24} simultaneously.

Figure 5 also depicts the forwarding of the monomials, at $t = 4$, from variable nodes v_{22} and v_{24} to their adjacent SA check nodes s_8 and s_{10} , respectively. Additionally, variable node v_{22} should also forward the monomial to its adjacent LDPC check node l_{18} . However, the path from l_{18} would either form a local LDPC cycle, or a global cycle of two extra transitions. Consequently, only the transitions to SA check nodes s_8 and s_{10} are relevant, and would be kept for further analysis.

As shown in Figure 5, at $t = 5$, s_8 forwards the monomial it received from v_{22} to its adjacent variable nodes v_5 , v_{12} , and v_{16} . Meanwhile, s_{10} forwards the monomial it received from v_{24} to its adjacent variable node, v_{13} . Considering the transitions of s_8 , variable node v_5 belongs to user U_1 . This is the same user that accommodates v_3 , the initiating variable node of the monomial at $t = 0$. Since v_5 and v_3 belong to the same user, if they share a common LDPC check node, the monomial would only need two more transitions to flow from v_5 to v_3 , via their common LDPC check node. Thus, the path from v_5 is considered as a candidate path of the shortest cycle analysis. Conversely, v_{12} and v_{16} belong to users U_2 and U_3 , respectively. This means that they do not share any common LDPC check nodes with v_3 . Hence, the monomial would need more than two transitions to flow from v_{12} and v_{16} to v_3 . It is also guaranteed that v_3 does not share the same SA check node with v_{12} and v_{16} , because otherwise, the monomial initiated by v_3 at $t = 0$, would have already landed on v_{12} and v_{16} at $t = 1$, which is not the case. Hence, the paths from s_8 to both v_{12} and v_{16} would require more transitions to reach v_3 , and are thus excluded from the candidate set. The same argument could be made for the path from s_{10} to v_{13} , which belongs to the variable nodes of user U_3 . In conclusion, the only relevant path at this time instant is the transition from s_8 to v_5 .

The transition from v_5 to LDPC check nodes l_4 and l_5 , at $t = 6$, is shown in Figure 6. As shown in the figure, l_4 is directly connected to v_3 . This means that at the next time instant, l_4 would forward the monomial to v_3 . On the other hand, l_5 does not exhibit a direction connection to v_3 . This means that l_5 would require at least two more time instants in comparison to l_4 , in order to send the monomial back to v_3 .

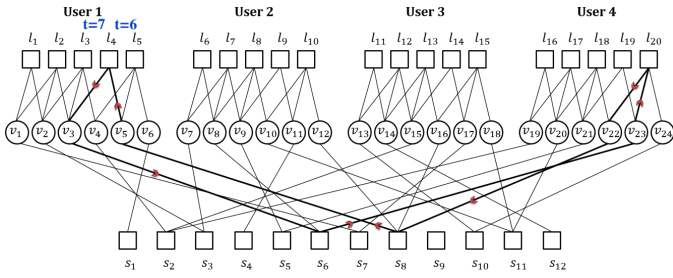


Fig. 6. Track of flow of beliefs at $t = 6, 7$, Case 1, on a SCRAM graph with $N_u = 4$ users, $n_{n_u} = 6$ symbols, and $N_s = 12$ slots

As a result, the path from l_5 is excluded from the candidate set of the shortest cycle.

Finally, at $t = 7$, as shown in Figure 6, l_4 forwards the monomial to v_3 . This completes one global cycle of eight transitions, that starts and terminates at variable node v_3 . In other words, the monomial transmitted by variable node v_3 , traverses the three-layer Tanner graph between SA check nodes, and variable and check nodes of the remaining users, and returns back to v_3 after eight transitions, resulting in a global cycle of length eight.

Now consider the second case left out at $t = 2$, where the monomial arrives at LDPC check node, l_{19} . As shown in Figure 7, at $t = 3$, l_{19} would forward the monomial to v_{21} . In return, at $t = 4$, v_{21} would forward it to SA check node s_5 , and to its adjacent LDPC check nodes, l_{17} and l_{18} . The forwarded monomial to the LDPC check nodes would either make a local cycle, or proceed further to a global cycle of two extra transitions, in comparison to the path to s_5 . Consequently, the paths to the LDPC check nodes are discarded, leaving only the transition to s_5 . At $t = 5$, s_5 forwards the monomial to variable node, v_9 , which belongs to user U_2 . Similar to the previous discussion in the first case, because v_9 and v_3 belong to different users, v_9 would require more than two more transitions to send the monomial back to v_3 . This means that the least cycle length due to this path would exceed eight, which is the length of the cycle traced from l_{20} in the first case. Therefore, case 1 is declared as the shortest global cycle, with a cycle length of eight.

Tracing the second case further from v_9 to l_7 to v_8 to s_6 to v_3 shows an example of a closed walk as depicted in Figure 8. Although the monomial returns back to v_3 after ten transitions, the walk is not considered a cycle because the starting and

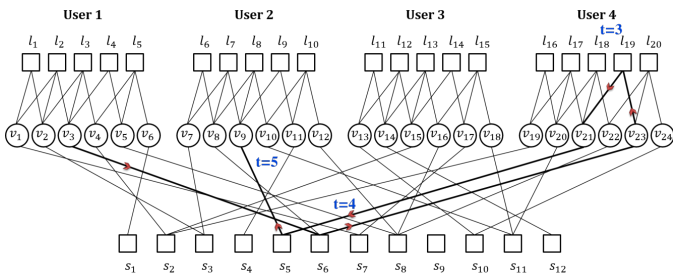


Fig. 7. Track of flow of beliefs at $t = 3, 4, 5$, Case 2, on a SCRAM graph with $N_u = 4$ users, $n_{n_u} = 6$ symbols, and $N_s = 12$ slots

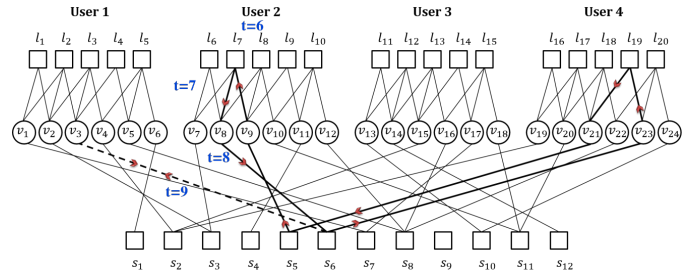


Fig. 8. Example of a closed walk at $t = 9$, Case 2, on a SCRAM graph with $N_u = 4$ users, $n_{n_u} = 6$ symbols, and $N_s = 12$ slots

ending edges are the same.

The example of the closed walk leads to an important observation, that is depicted in Figure 9. The figure shows the further tracking of the monomial after it arrives at v_9 at $t = 5$, till it reaches v_3 , after a global cycle of length 12. This means that this part of the analysis considers the case where the monomial at v_9 would follow a different path, than the path that lead to the closed walk. For this path, the monomial is forwarded from v_9 to l_7 at $t = 6$, and from l_7 to v_7 at $t = 7$. After that, the monomial is forwarded from v_7 to s_3 , and from s_3 to v_2 , at $t = 8$ and $t = 9$, respectively. The major observation here is that due to the fact that after six transitions from the initial phase at $t = 0$, the monomial landed on a variable node (v_9), that does not belong to the variable node set of the initiating variable node (v_3), the monomial required at least four more transitions ($t = 6 \rightarrow t = 9$), in order to be able to leave the variable node set of the variable node (v_9) that it landed on, and land on a variable node (v_2), that belongs to the variable node set of the initiating variable node (v_3). Now because v_2 and v_3 have a common LDPC check node (l_2), after two more time instants, that is at $t = 11$, the monomial would arrive at v_3 via passing by l_2 . Consequently, the total cycle length of this global cycle is $6 + 4 + 2 = 12$. Any other attempt to reach v_3 from v_9 , would either go through a closed walk, or a global cycle of length at least 12.

To wrap up the analysis, the first six time slots of a global cycle involve three crucial pair of transitions. The first pair represents the transition from the initiating variable node that belongs to a certain user, to a second variable node that belongs to a different user, via passing by a common SA check node. The second pair involves a transition from the second variable node, to another variable node that belongs to the

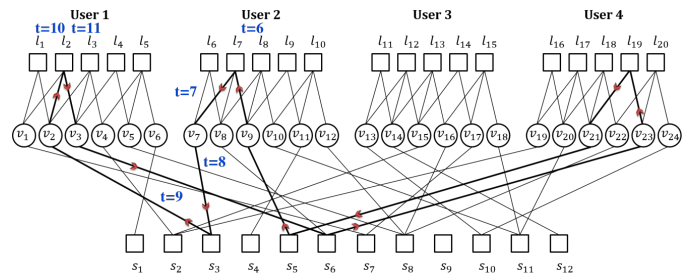


Fig. 9. Track of flow of beliefs at $t = 6, 7, 8, 9, 10, 11$, Case 2, on a SCRAM graph with $N_u = 4$ users, $n_{n_u} = 6$ symbols, and $N_s = 12$ slots

same user, via passing by a shared LDPC check node. For the third pair of transitions, the monomial is forwarded from the receiving variable node from the previous pair, to another variable node in a different user set, via passing by a common SA check node. These three pairs of transitions are crucial, and require six time slots. Two possible scenarios could arise after the landing on the last variable node from the last pair.

The first scenario corresponds to the case where the landed on variable node belongs to the same user of the initiating variable node at $t = 0$. In this case, if the two variable nodes share a common LDPC check node, then only one pair of transitions is required for the information to go back to its initiating variable node. Consequently, the total cycle length of the global cycle is eight. If on the other hand, the two variable nodes do not have a common LDPC check node, then at least two more pairs of transitions are required to complete the cycle. In this case, the cycle length is at least 10.

The second scenario corresponds to the case where the landed on variable node does not belong to the same user as the initiating variable node. In this case, as was discussed in the last example, at least two more pairs of transitions are required for the monomial to leave the current user set, and land on a variable node within the user set of the initiating variable node. After these two more pairs, the situation translates to the first scenario, which means another one or more transitions is required to finish the cycle. As a result, this situation requires at least three more pairs of transitions, in addition to the crucial three transitions. Consequently, the least cycle length from the second scenario is 12.

From the above discussion, it can be deduced that the shortest length of a global cycle on the SCRAM Tanner graph is at least eight. This indicates that the global girth is given by $g_{global} \geq 8$. If any of the adopted LDPC codes, has a local girth, g_{local} , that is less than eight, the overall SCRAM girth would match the smaller girth, whether it is the local girth of the individual LDPC codes, or the global girth of at least eight. Consequently, it can be deduced that the overall SCRAM girth is given by $g_{SCRAM} \geq \min(8, g_{local})$.

V. A PROPOSED GRAPHICAL CORRELATION-BASED METHOD FOR COUNTING THE NUMBER OF GLOBAL 8-CYCLES ON THE SCRAM THREE-LAYER TANNER GRAPH

As mentioned previously, the mapping of the SCRAM three-layer Tanner graph to a hybrid matrix enables the utilization of the Full-Cycle or the Half-Cycle algorithms, initially proposed for classical LDPC codes, in computing the cycle profile of SCRAM. However, the complexity of these algorithms grows exponentially in the number of users and the number of LDPC symbols per user. In the previous section, it was shown that the least global cycle length on a SCRAM three-layer Tanner graph was found to be eight. In this section, a graphical method that counts the number of global 8-cycles on the SCRAM three-layer Tanner graph is proposed. Instead of computing the full-cycle profile, the proposed algorithm focuses on the global 8-cycles, as they are provisioned to have a more detrimental effect on the convergence of the joint SCRAM decoding.

As discussed in the previous section, a global cycle of length eight, on the SCRAM three-layer Tanner graph, involves four transition pairs. The first pair represents the hopping from the

initiating variable node of one user, to a variable node that belongs to a different user, via a common SA check node. The second pair corresponds to a hop from the receiving variable node, to another variable node within its user set, via a common LDPC check node. The third pair involves the return trip from the last variable node, back to another variable node within the set of the initiating user, via a common SA check node. Finally, the fourth pair corresponds to the hopping from the receiving variable node, to the initiating variable node, via a common LDPC check node. For simplicity, in the sequel, two variable nodes, that belong to the same user, are referred to as connected variable nodes, if and only if there is a common LDPC check node, that is simultaneously connected to each one of them, via a single edge. With this definition, it can be summed up that a global cycle of length eight involves two connected variable nodes on one user set, two connected variable nodes on a different user set, and two common SA check nodes, shared by the four variable nodes.

In order to count the total number of global 8-cycles, the algorithm loops over all the variable nodes, and calculates the number of global 8-cycles that pass through each one of them. For every iteration, the user that accommodates the variable node of interest is referred to as the primary user, while all the remaining users are referred to as the secondary users. In addition, the variable node of interest is denoted by $v_1^{(p)}$, which denotes the first primary variable node. Because a global 8-cycle involves two connected variable nodes on one user set, the connected variable node to $v_1^{(p)}$ is denoted by $v_2^{(p)}$, and their connecting LDPC check node is referred to as $l^{(p)}$. In a similar fashion, for the second connected pair of variable nodes of the global 8-cycle, the first secondary variable node, the second secondary variable node, and their connecting LDPC check node, on the secondary user set, are referred to as, $v_1^{(s)}$, $v_2^{(s)}$, and $l^{(s)}$, respectively. Finally the shared SA check node that connects the first primary- and the first secondary variable nodes is denoted by $s_1^{(p,s)}$. Similarly, the shared SA check node that connects the second primary- and the second secondary variable nodes is denoted by $s_2^{(p,s)}$.

For a SCRAM three-layer Tanner graph with N_v variable nodes, the proposed algorithm calculates the number of global 8-cycles, $C_8^{(v_{n_v})}$ that pass through variable node v_{n_v} , $\forall n_v = 1, \dots, N_v$, and accumulates it to the global 8-cycle counter, $C_8^{(global)}$. For every iteration, the first primary variable node, $v_1^{(p)}$ is assigned to v_{n_v} . Let $A_{v_1^{(p)}}^{(L)}$, be the set of LDPC check nodes, connected to the first primary variable node. While the outer loop of the algorithm loops over the variable nodes, the first inner loop should loop over their adjacent LDPC check nodes. For every iteration on the set of adjacent LDPC check nodes, the check node of interest is referred to as $l^{(p)}$, which denotes the primary LDPC check node. At this stage, the algorithm starts a new nested loop, that iterates over the edges of the primary LDPC check node. Let $A_{l^{(p)}}$, denote the set of variable nodes connected to the primary LDPC check node, $l^{(p)}$. Moreover, let $A_{l^{(p)}/v_1^{(p)}}$, denote the set of adjacent variable nodes of the primary LDPC check node, except the first primary variable node. For every iteration over $A_{l^{(p)}/v_1^{(p)}}$, the selected variable node is referred to as $v_2^{(p)}$, which denotes

the second primary variable node.

Now that $v_1^{(p)}$ and $v_2^{(p)}$ have been identified, the next step is to identify their adjacent SA check nodes. Let $A_{v_1^{(p)}}^{(S)}$, and $A_{v_2^{(p)}}^{(S)}$, be the set of SA check nodes, connected to $v_1^{(p)}$ and $v_2^{(p)}$, respectively. Without loss of generality, due to the fact that every modulated symbol is transmitted only once, each of the two sets includes a single SA check node. This means that the first constituent SA check node, $s_1^{(p,s)}$, and the second constituent SA check node, $s_2^{(p,s)}$, are the only elements in $A_{v_1^{(p)}}^{(S)}$ and $A_{v_2^{(p)}}^{(S)}$, respectively.

To complete the constituents of the global 8-cycle, the two secondary variable nodes are to be identified. These variable nodes should be colliding on the pair of constituent SA check nodes, $s_1^{(p,s)}$, and $s_2^{(p,s)}$. Moreover, they both should belong to the same secondary user. Furthermore, they should be connected via a common LDPC check node. As a first step, all the colliding variable nodes on $s_1^{(p,s)}$, and $s_2^{(p,s)}$ have to be identified. Let $A_{s_1^{(p,s)}}$, and $A_{s_2^{(p,s)}}$, denote the set of variable nodes, colliding at $s_1^{(p,s)}$, and $s_2^{(p,s)}$, respectively. Because the primary variable nodes have to be excluded from the potential candidates of secondary variable nodes, let $A_{s_1^{(p,s)}/v_1^{(p)}}$, and $A_{s_2^{(p,s)}/v_2^{(p)}}$, denote the set of variable nodes that collide at $s_1^{(p,s)}$, excluding $v_1^{(p)}$, and the set of variable nodes that collide at $s_2^{(p,s)}$, excluding $v_2^{(p)}$, respectively. At this stage, the algorithm loops over the variable nodes in $A_{s_1^{(p,s)}/v_1^{(p)}}$, and $A_{s_2^{(p,s)}/v_2^{(p)}}$, and for every iteration denotes the selected variable node from $A_{s_1^{(p,s)}/v_1^{(p)}}$ and $A_{s_2^{(p,s)}/v_2^{(p)}}$ as the first secondary variable node, $v_1^{(s)}$, and the second secondary variable node, $v_2^{(s)}$, respectively.

If the two secondary variable nodes do not belong to the same user, their combination should be excluded. On the other hand, if they belong to the same user set, the algorithm proceeds to check if they are connected, and if so, how many LDPC check nodes they have in common. This can be done via analyzing the parity check matrix of the underlying LDPC code. When two variable nodes, share a common LDPC check node, the parity check matrix possesses a value of one, at the row intersection of the respective LDPC check node, and the two column indices of the two variable nodes. Thus, the element-wise multiplication, of the two corresponding columns of the variable nodes of interest, would yield ones, at the row indices of the LDPC check nodes that the two variable nodes are simultaneously connected to. Moreover, the summation of the elements within the resulting column after the multiplication, yields the total number of LDPC check nodes, that the two variable nodes share in common. Each common LDPC check node, represents a potential transition pair between the two variable nodes, to close the global 8-cycle. In other words, for every common LDPC check node between the secondary variable nodes, the cycle counter is incremented by one. If on the other hand, the two secondary variable nodes, do not share any common LDPC check nodes, then this pair of secondary variable nodes is excluded from the potential 8-cycle constituent candidates.

It is worth pointing out that the indices of the variable

nodes, and LDPC check nodes within the joint three-layer Tanner graph, are different from their corresponding indices within the underlying parity check matrix of the adopted LDPC code. For that reason, a simple mapping between the indices on the joint Tanner graph, and the respective indices within the underlying LDPC code, has to be made. Assuming, that all the N_u users, adopt identical LDPC codes, with n_{n_u} variable nodes, and m_{n_u} LDPC check nodes each, then for $n_v = 1, \dots, N_v$, such that N_v is the total number of variable nodes in the joint Tanner graph, the corresponding user index, n_u , to which variable node, v_{n_v} , belongs, is given by $n_u = \lceil \frac{n_v}{n_{n_u}} \rceil$. Moreover, the respective index, i , of the variable node within the underlying LDPC code can be computed as, $i = \text{mod}(n_v - 1, n_{n_u}) + 1$. This means that variable node, v_{n_v} , within the joint Tanner graph, corresponds to variable node, v_i , within the underlying LDPC code, of user, U_{n_u} . Similarly, for $n_l = 1, \dots, N_l$, such that N_l represents the total number of LDPC check nodes in the joint Tanner graph, LDPC check node, l_{n_l} , within the joint Tanner graph, corresponds to LDPC check node, l_j , within the underlying LDPC code of user, U_{n_u} , such that, $n_u = \lceil \frac{n_l}{m_{n_u}} \rceil$, and $j = \text{mod}(n_l - 1, m_{n_u}) + 1$. For the case of non-identical LDPC codes, the mapping is straightforward, taking into consideration the respective number of variable nodes, n_{n_u} , and LDPC check nodes, m_{n_u} , within the parity check matrix, $\mathbf{H}_{\text{LDPC}}^{(n_u)}$, of user, U_{n_u} .

For every common LDPC check node between, $v_1^{(s)}$ and $v_2^{(s)}$, the 8-cycle counter, $C_8^{(v_1^{(p)})}$, of the global 8-cycles that pass through the first primary variable node, $v_1^{(p)}$, should be incremented by one. At this point, the algorithm reverts to the second inner loop, checking if there are further variable nodes, connected to the primary LDPC check node, in the set, $A_{l^{(p)}/v_1^{(p)}}$, of adjacent variable nodes, of the current primary LDPC check node, $l^{(p)}$, excluding the current first primary variable node, $v_1^{(p)}$. After terminating the second inner loop, the algorithm proceeds to check if there are further iterations required in the first inner loop. This means that the algorithm has to check whether or not there are further LDPC check nodes, connected to the first primary variable node. Before proceeding to the outer loop, to investigate a new primary variable node, the total 8-cycle counter, $C_8^{(\text{global})}$, should be incremented by the 8-cycle counter, $C_8^{(v_1^{(p)})}$, of the first primary variable node, $v_1^{(p)}$. A crucial consideration for the next iterations in the outer loop, is to exclude any potential 8-cycle, that involves the previously investigated primary variable nodes, in order to avoid duplications.

For illustration, consider the example shown in Figure 10, with four users, adopting the same LDPC codes as the previous examples. The system incorporates 12 channel access slots, and the users access the channel by means of random access. Assume that the objective is to track the potential global 8-cycles, that pass through variable nodes v_3 and v_5 , that belong to user U_1 . As a result, user U_1 , is denoted by the primary user, while users, U_2 , U_3 , and U_4 , are referred to as the secondary users. Moreover, the first and second primary variable nodes, $v_1^{(p)}$ and $v_2^{(p)}$, are respectively assigned to v_3 and v_5 . Consequently, the first and second constituent SA

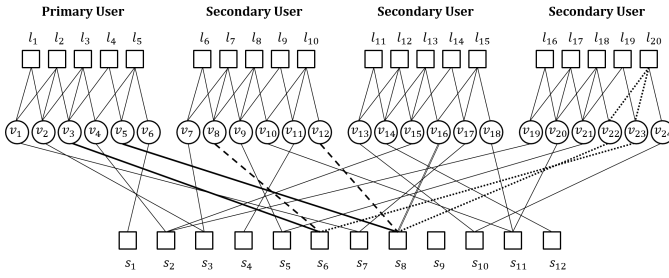


Fig. 10. Example of algorithmic tracking of 8-cycles between four users on a SCRAM Tanner graph with twelve SA slots, Case 2

check nodes, $s_1^{(p,s)}$ and $s_2^{(p,s)}$, should be assigned to s_6 and s_8 , respectively. Concerning the first secondary variable node, the set $A_{s_1^{(p,s)}/v_1^{(p)}}$, of adjacent variable nodes, of the first constituent SA check node, s_6 , excluding the first primary variable node, v_3 , includes both v_8 and v_{23} , which belong to users, U_2 , and U_4 , respectively. This means that there are two potential candidates for the first secondary variable node, $v_1^{(s)}$. Similarly, the set $A_{s_2^{(p,s)}/v_2^{(p)}}$, of adjacent variable nodes, of the second constituent SA check node, s_8 , excluding the second primary variable node, v_5 , includes v_{12} , v_{16} , and v_{22} , which belong to users, U_2 , U_3 , and U_4 , respectively. This means that there are three potential candidates for the second secondary variable node, $v_2^{(s)}$. As a result, the algorithm should include a new nested loop, that investigates all the possible candidate pairs of first and second secondary variable nodes.

The example tackles three possible scenarios that could occur during the nested loop investigation. The first scenario is concerned with v_{16} , as one of the potential candidates of $v_2^{(s)}$. Due to the fact that v_{16} belongs to user U_3 , and none of the two potential candidates of $v_1^{(s)}$, belongs to U_3 , no possible pair that includes v_{16} , could close a global 8-cycle. Consequently, v_{16} should be excluded.

The second scenario investigates the pair of v_8 and v_{12} , such that v_8 represents the first potential secondary variable node, $v_1^{(s)}$, while v_{12} represents the second potential secondary variable node, $v_2^{(s)}$. Because both v_8 and v_{12} , belong to the same user, U_2 , they could close a global 8-cycle, provided that they are connected via one or more LDPC check nodes. Analyzing the underlying parity check matrix, as described previously, it can be shown that there is no common LDPC check node, that connects v_8 and v_{12} . As a result, the least cycle length that can be constituted by including both v_8 and v_{12} , is certainly greater than eight.

As for the third scenario, the pair of v_{23} and v_{22} , such that v_{23} represents the first potential secondary variable node, $v_1^{(s)}$, while v_{22} represents the second potential secondary variable node, $v_2^{(s)}$, is to be investigated. Similar to the previous scenario, because both v_{23} and v_{22} , belong to the same user, U_4 , they could close a global 8-cycle, provided that they are connected via one or more LDPC check nodes. Analyzing the underlying parity check matrix, this time shows that v_{23} and v_{22} , are connected via LDPC check node, l_{20} . Consequently, the pair of v_{23} and v_{22} , closes a global 8-cycle, that passes through v_3 and v_5 , and leads to incrementing the 8-cycle

counter, $C_8^{(v_3)}$, of variable node, v_3 , by one.

VI. RESULTS

In the previous section, a graphical algorithm that computes the number of global 8-cycles, in the three-layer Tanner graph of a SCRAM system was proposed. The proposed algorithm is pillared on the thoroughly investigated structure of the global 8-cycle that was presented in section IV. This section extends the results presented in Section III-C, to include the algorithmic calculation of the number of global 8-cycles, in a SCRAM system, with $N_u = 4$ users, $N_s = 8640$ slots, and the (4320, 2160) DVB-NGH [34] LDPC code. The aim of this section is to analyze and validate the results obtained from the proposed algorithm, by comparing them to the total number of 8-cycles, from the cycle profile of SCRAM.

Table III is thus regarded as an extension to the results in Table II, with an extra column that includes the number of global 8-cycles, in the SCRAM three-layer Tanner graph, obtained from the proposed global 8-cycle counting algorithm. Here again, the first row depicts the cycle profile of the (4320, 2160) DVB-NGH [34] LDPC code. The second row shows the number of global 8-cycles, in the SCRAM three-layer Tanner graph, obtained from the proposed global 8-cycle counting algorithm. In addition, it shows the cycle profile of the SCRAM system, obtained from the Half-Cycle [31] counting algorithm of the SCRAM hybrid matrix.

Because The investigated SCRAM system incorporates $N_u = 4$ users, it has a number of local LDPC 8-cycles, that corresponds to four times the number of 8-cycles, of a single LDPC code. This means that, the SCRAM Tanner graph has a total of 6233360 local LDPC 8-cycles. Meanwhile, as shown in the table, the results of the proposed global 8-cycle counting algorithm, indicate that the random access scheme, adds additional 725 global 8-cycles. This means that the SCRAM Tanner graph, has a total of 6234085, cycles of length eight, which complies with the number of 8-cycles, obtained from the cycle profile of the Half-Cycle counting algorithm of the mapped SCRAM hybrid matrix.

The results herein show that the number of 6-cycles in the SCRAM three-layer Tanner graph, corresponds to four times that of the NGH LDPC code. This indicates that all the 6-cycles, in the SCRAM system, are local LDPC cycles. Consequently, the hypothesis that the adopted channel scheme does not add cycles of length six, and the claim of Section IV, that the shortest global cycle length is eight, have been verified. Moreover, the results of the 8-cycles verify the validity of the proposed global 8-cycle counting algorithm of the SCRAM three-layer Tanner graph. Because the proposed algorithm has significantly lower complexity than the Half-Cycle counting algorithm, it can be utilized to compute the number of global 8-cycles, of the SCRAM system.

TABLE III
ALGORITHMIC 8-CYCLE RESULTS OF SCRAM, WITH $N_u = 4$ USERS,
ADOPTING THE (4320, 2160) DVB-NGH LDPC CODE, WITH RANDOM
ACCESS, ON A CHANNEL WITH $N_s = 8640$ SLOTS

	C_6	C_8	Global 8-Cycles
(4320, 2160) DVB-NGH LDPC	31200	1558340	
SCRAM, with $N_u = 4$ users	124800	6234085	725

VII. CONCLUSIONS

In this paper, a graphical correlation-based method that counts the number of global 8-cycles on the SCRAM (Slotted Coded Random Access Multiplexing) three-layer Tanner graph is proposed. The essence of SCRAM lies in its hybrid decoding structure, that jointly resolves the collisions and decodes the Low Density Parity Check (LDPC) codewords, in a similar analogy to Belief Propagation Decoding, on a joint three-layer Tanner graph. This paper leverages the analogy between the two-layer Tanner graph of classical LDPC codes, and the three-layer Tanner graph of the proposed SCRAM, in order to further optimize the performance of SCRAM.

The paper first introduces the necessary procedure required to utilize the leading state-of-the-art tools that compute the cycle profile of classical LDPC codes, to compute the cycle profile of SCRAM. The paper also derives a lower bound on the shortest cycle length (girth) of a SCRAM system, with arbitrary number of accommodated users and deployed LDPC codes. In essence, the paper proposes a novel graphical approach that scans the three-layer Tanner graph of SCRAM, in search for the cycles of girth length. The results presented herein show that the proposed cycle-counting approach yields exactly the same results as the conventional LDPC tools at much lower complexity cost. Future implications include the utilization of the analysis tools proposed herein, in order to devise an optimized SCRAM system with bounds on the cycle profile as the optimization cost function.

REFERENCES

- [1] M. H. Miraz, M. Ali, P. S. Excell, and R. Picking, "A review on internet of things (IoT), internet of everything (IoE) and internet of nano things (IoNT)," *2015 Internet Technologies and Applications (ITA)*, pp. 219–224, 2015.
- [2] W. Saad, M. Bennis, and M. Chen, "A vision of 6G wireless systems: Applications, trends, technologies, and open research problems," *IEEE network*, vol. 34, no. 3, pp. 134–142, 2019.
- [3] M. Z. Chowdhury, M. Shahjalal, S. Ahmed, and Y. M. Jang, "6G wireless communication systems: Applications, requirements, technologies, challenges, and research directions," *IEEE Open Journal of the Communications Society*, vol. 1, pp. 957–975, 2020.
- [4] Z. Ding, M. Peng, and H. V. Poor, "Cooperative non-orthogonal multiple access in 5G systems," *IEEE Communications Letters*, vol. 19, no. 8, pp. 1462–1465, 2015.
- [5] S. R. Islam, N. Avazov, O. A. Dobre, and K.-S. Kwak, "Power-domain non-orthogonal multiple access (NOMA) in 5G systems: Potentials and challenges," *IEEE Communications Surveys & Tutorials*, vol. 19, no. 2, pp. 721–742, 2016.
- [6] P. V. Reddy, S. Reddy, S. Reddy, R. D. Sawale, P. Narendar, C. Dugineni, and H. B. Valiveti, "Analytical review on OMA vs. NOMA and challenges implementing NOMA," in *2021 2nd International Conference on Smart Electronics and Communication (ICOSEC)*. IEEE, 2021, pp. 552–556.
- [7] S. Srivastava and P. P. Dash, "Non-orthogonal multiple access: Procession towards 5G and 6G," in *2021 IEEE 2nd International Conference on Applied Electromagnetics, Signal Processing, & Communication (AESPC)*. IEEE, 2021, pp. 1–4.
- [8] O. Maraqa, A. S. Rajasekaran, S. Al-Ahmadi, H. Yanikomeroğlu, and S. M. Sait, "A survey of rate-optimal power domain NOMA with enabling technologies of future wireless networks," *IEEE Communications Surveys & Tutorials*, vol. 22, no. 4, pp. 2192–2235, 2020.
- [9] I.-H. Lee and H. Jung, "User selection and power allocation for downlink NOMA systems with quality-based feedback in rayleigh fading channels," *IEEE Wireless Communications Letters*, vol. 9, no. 11, pp. 1924–1927, 2020.
- [10] P. Gupta and D. Ghosh, "User fairness based energy efficient power allocation for downlink cellular NOMA system," in *2020 5th International Conference on Computing, Communication and Security (ICCCS)*. IEEE, 2020, pp. 1–5.
- [11] A. Jehan and M. Zeeshan, "Comparative performance analysis of code-domain NOMA and power-domain NOMA," in *2022 16th International Conference on Ubiquitous Information Management and Communication (IMCOM)*. IEEE, 2022, pp. 1–6.
- [12] Z. Liu and L.-L. Yang, "Sparse or dense: A comparative study of code-domain NOMA systems," *IEEE Transactions on Wireless Communications*, vol. 20, no. 8, pp. 4768–4780, 2021.
- [13] S. Chen, B. Ren, Q. Gao, S. Kang, S. Sun, and K. Niu, "Pattern division multiple access—a novel nonorthogonal multiple access for fifth-generation radio networks," *IEEE Transactions on Vehicular Technology*, vol. 66, no. 4, pp. 3185–3196, 2016.
- [14] H. Nikopour and H. Baligh, "Sparse code multiple access," in *2013 IEEE 24th Annual International Symposium on Personal, Indoor, and Mobile Radio Communications (PIMRC)*. IEEE, 2013, pp. 332–336.
- [15] M. Al-Imari, P. Xiao, M. A. Imran, and R. Tafazolli, "Uplink non-orthogonal multiple access for 5G wireless networks," in *2014 11th international symposium on wireless communications systems (ISWCS)*. IEEE, 2014, pp. 781–785.
- [16] S. Chaturvedi, Z. Liu, V. A. Bohara, A. Srivastava, and P. Xiao, "A tutorial on decoding techniques of sparse code multiple access," *IEEE Access*, 2022.
- [17] N. Zhang and X. Zhu, "A hybrid grant NOMA random access for massive MTC service," *IEEE Internet of Things Journal*, vol. 10, no. 6, pp. 5490–5505, 2022.
- [18] S. Gollakota and D. Katabi, "Zigzag decoding: Combating hidden terminals in wireless networks," in *Proceedings of the ACM SIGCOMM 2008 conference on Data communication*, 2008, pp. 159–170.
- [19] A. S. Tehrani, A. G. Dimakis, and M. J. Neely, "Sigsag: Iterative detection through soft message-passing," *IEEE Journal of Selected Topics in Signal Processing*, vol. 5, no. 8, pp. 1512–1523, 2011.
- [20] J. Xiao, J. Hu, and K. Han, "Low complexity expectation propagation detection for scma using approximate computing," in *2019 IEEE Global Communications Conference (GLOBECOM)*. IEEE, 2019, pp. 1–6.
- [21] P. Herath, A. Haghghat, and L. Canonne-Velasquez, "A low-complexity interference cancellation approach for NOMA," in *2020 IEEE 91st Vehicular Technology Conference (VTC2020-Spring)*. IEEE, 2020, pp. 1–5.
- [22] N. Iswarya and L. Jayashree, "A survey on successive interference cancellation schemes in non-orthogonal multiple access for future radio access," *Wireless Personal Communications*, vol. 120, no. 2, pp. 1057–1078, 2021.
- [23] B. Ling, C. Dong, J. Dai, and J. Lin, "Multiple decision aided successive interference cancellation receiver for NOMA systems," *IEEE Wireless Communications Letters*, vol. 6, no. 4, pp. 498–501, 2017.
- [24] B. Ren, X. Yue, W. Tang, Y. Wang, S. Kang, X. Dai, and S. Sun, "Advanced IDD receiver for PDMA uplink system," in *2016 IEEE/CIC International Conference on Communications in China (ICCC)*. IEEE, 2016, pp. 1–6.
- [25] S. Nafie, J. Robert, and A. Heuberger, "SCRAM: A novel approach for reliable ultra-low latency m2m applications," in *2018 IEEE 88th Vehicular Technology Conference (VTC-Fall)*. IEEE, 2018, pp. 1–5.
- [26] A. Munari, F. Clazzer, and G. Liva, "Multi-receiver ALOHA systems—a survey and new results," in *Communication Workshop (ICCW), 2015 IEEE International Conference on*. IEEE, 2015, pp. 2108–2114.
- [27] R. Gallager, "Low-density parity-check codes," *IRE Transactions on information theory*, vol. 8, no. 1, pp. 21–28, 1962.
- [28] D. J. MacKay and R. M. Neal, "Near shannon limit performance of low density parity check codes," *Electronics letters*, vol. 33, no. 6, pp. 457–458, 1997.
- [29] R. Tanner, "A recursive approach to low complexity codes," *IEEE Transactions on information theory*, vol. 27, no. 5, pp. 533–547, 1981.
- [30] M. Karimi and A. H. Banihashemi, "Message-passing algorithms for counting short cycles in a graph," *IEEE Transactions on Communications*, vol. 61, no. 2, pp. 485–495, 2012.
- [31] J. Li, S. Lin, and K. Abdel-Ghaffar, "Improved message-passing algorithm for counting short cycles in bipartite graphs," in *2015 IEEE International Symposium on Information Theory (ISIT)*. IEEE, 2015, pp. 416–420.
- [32] S. J. Johnson, "Introducing low-density parity-check codes," *University of Newcastle, Australia*, vol. 1, p. 2006, 2006.
- [33] X. Xiao, B. Vasić, S. Lin, K. Abdel-Ghaffar, and W. E. Ryan, "Reed-solomon based quasi-cyclic LDPC codes: Designs, girth, cycle structure, and reduction of short cycles," *IEEE Transactions on Communications*, vol. 67, no. 8, pp. 5275–5286, 2019.
- [34] D. Gomez-Barquero, C. Douillard, P. Moss, and V. Mignone, "DVB-NGH: The next generation of digital broadcast services to handheld devices," *IEEE Transactions on Broadcasting*, vol. 60, no. 2, pp. 246–257, 2014.